Compact Surface Fano States Embedded in the Continuum of Waveguide Arrays

Steffen Weimann,[1] Yi Xu,[2] Robert Keil,[1] Andrey E. Miroshnichenko,[2] Andreas Tünnermann,[1] Stefan Nolte,[1] Andrey A. Sukhorukov,[2] Alexander Szameit,[1] and Yuri S. Kivshar[2]

[1]*Institute of Applied Physics, Abbe Center of Photonics, Friedrich-Schiller-Universität Jena, Max-Wien-Platz 1, 07743 Jena, Germany*

[2]*Nonlinear Physics Centre, Research School of Physics and Engineering, Australian National University, Canberra, Australian Capital Territory 0200, Australia*

(Received 10 June 2013; published 10 December 2013)

We describe theoretically and observe experimentally the formation of a surface state in a semi-infinite waveguide array with a side-coupled waveguide, designed to simultaneously achieve Fano and Fabry-Perot resonances. We demonstrate that the surface mode is compact, with all energy concentrated in a few waveguides at the edge and no field penetration beyond the side-coupled waveguide position. Furthermore, we show that by broadening the spectral band in the rest of the waveguide array it is possible to suppress exponentially localized modes, while the Fano state having the eigenvalue embedded in the continuum is preserved.

DOI: 10.1103/PhysRevLett.111.240403 PACS numbers: 03.65.Nk, 42.65.−k, 42.79.Gn

The wave localization at surfaces and interfaces is a fundamental physical phenomenon, associated with the presence of spatial inhomogeneity. Common examples are interfaces between two different media, which include surface plasmon-polaritons at a dielectric-metal interface [1,2], Dyakonov states at isotropic-anisotropic interfaces [3], and Tamm states at homogeneous-periodic media interfaces [4]. Although of different origin, these modes share the same property: the exponential decay away from the interface. Such a spatial localization profile usually requires that the eigenfrequencies of the surface states lie outside the band of the propagating spatially extended states. Otherwise, there will be a resonant interaction between the exponential—but nonzero—tails of the localized states and these extended states.

Remarkably, in their seminal paper von Neumann and Wigner [5] explicitly constructed a potential that supports so-called "bound states in the continuum" (BIC), i.e., a particular localized mode with the eigenfrequency inside the band of extended states. Since then, the peculiar concept of BIC has attracted a lot of attention in various branches of physics [6,7], reaching a climax with the direct observation of an electronic bound state above a potential well due to Bragg reflection in semiconductor heterostructures [8]. In the optical domain, it was shown that BIC can be generated in photonic crystals, plasmonic nanostructures, quantum dot systems, and optical waveguide arrays [9–21]. The first true observation of a BIC in any system was carried out in an optical system: a planar optical waveguide array with two side-coupled defects, in which an in-band defect state is formed by virtue of symmetry [22]. Recently, a special design of a one-dimensional (1D) waveguide array with modulated intersite coupling was suggested in order to obtain "surface BIC" [23].

The phenomenon of Fano resonance [24] provides a universal means for obtaining bound states in the continuum and has been encountered in many different optical settings [25], e.g., through the addition of side-coupled waveguides or cavities [26]. The destructive interference occurring at Fano resonance is responsible for light trapping studied in photonic crystal waveguides between two side-coupled defects [27–29], at a cavity placed near the waveguide termination [30], and is predicted for waveguide arrays with side-coupled waveguides [10].

In this Letter, we present theoretical analysis and experimental observation of the formation of surface states trapped due to Fano resonance. To this end, we employ an optical system: an array of evanescently coupled waveguides with a side-coupled waveguide close to the lattice edge. We show that the surface Fano modes are "compact"; i.e., there is no wave penetration beyond the location of the side-coupled waveguide, in agreement with the principles of Fano resonance based on complete destructive interference in transmission. Moreover, we also demonstrate that conventional defect modes with exponentially localized tails, which are also found in the system, can be suppressed while the surface Fano mode remains trapped. This suppression is realized by increasing the waveguide coupling past the side-coupled waveguide. Such a selective manipulation of modes sensitive to their localization mechanism may find applications in various physical contexts, since the Fano resonance is a general wave interference phenomenon. We study the formation of Fano surface localized modes in an optical waveguide array with a single side-coupled waveguide as shown in Fig. 1. In Fano's original work, two configurations interacted. One configuration is the continuous band of infinitely extended vacuum states, which is here given by the quasicontinuous band of the supermodes of the 1D waveguide chain. The other configuration was a discrete autoionizing energy level, which is here given as the fundamental mode of the additional waveguide. In analogy to the atomic physics

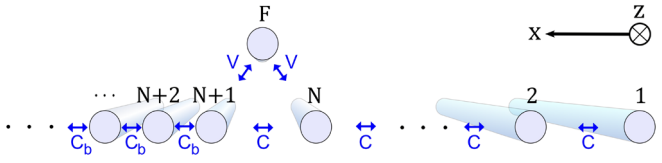

FIG. 1 (color online). Sketch of a semi-infinite waveguide array, where a side-coupled waveguide is introduced to provide the Fano resonance.

context, this side-coupled waveguide is called the "autoionizing" waveguide (AW). The waveguide structure consists of a 1D chain of identical waveguides. The propagation direction and the transverse direction are z and x, respectively. The chain is coupled to the AW with strength V. The part containing the waveguides 1 to N is a resonator region. Here, the coupling coefficient between neighboring waveguides is C. We consider the general situation when the coupling strength C_b in the "background" region, i.e., the semi-infinite array section containing the waveguides $N+1, N+2, \ldots$, is different. As we demonstrate below, the variation of the background coupling enables the selective manipulation of Fano modes and regular exponentially localized modes.

We model the evolution of the optical mode amplitudes along the propagation direction using a coupled-mode approach with nearest-neighbor coupling [31],

$$\begin{aligned}
&i\frac{\partial\psi_j}{\partial z} + C(\psi_{j+1} + \psi_{j-1}) = 0, \quad 1 \le j < N,\\
&i\frac{\partial\psi_F}{\partial z} + V(\psi_{N+1} + \psi_N) = 0,\\
&i\frac{\partial\psi_N}{\partial z} + V\psi_F + C(\psi_{N-1} + \psi_{N+1}) = 0,\\
&i\frac{\partial\psi_{N+1}}{\partial z} + V\psi_F + C\psi_N + C_b\psi_{N+2} = 0,\\
&i\frac{\partial\psi_j}{\partial z} + C_b(\psi_{j+1} + \psi_{j-1}) = 0, \quad j > N+1,
\end{aligned} \tag{1}$$

where ψ_j describes the optical mode amplitude in the jth waveguide. We put $\psi_0 \equiv 0$ due to the array termination. In this formulation, the spectrum is centered around the propagation constant of an isolated waveguide.

The waveguide F is a defect to the 1D chain, and plane waves incident on the triangle of waveguides exhibit a transmission that is dependent on the value of their propagation constant β. It is convenient to represent the field inside the resonator region ($n = 1, \ldots, N$) in terms of incident and reflected waves as $\psi_n = \exp(i\beta z)[\exp(i(n-N)\kappa) + R\exp(-i(n-N)\kappa)]$ and in the background region ($n = N+1, N+2, \ldots$) the field will be the transmitted wave $\psi_n = \exp(i\beta z)T\exp[i(n-N-1)\kappa_b]$, where the linear dispersion relations are $\beta = 2C\cos(\kappa) = 2C_b\cos(\kappa_b)$. One finds from Eq. (1) with $C_b = C$ that the transmission amplitude is

$$T = 2i\sin(\kappa)[2\cos(\kappa)C^2 + V^2]CD^{-1} \tag{2}$$

where $D = C^3e^{i\kappa} - C^2C_be^{-i(2\kappa+\kappa_b)} + 2CV^2e^{i\kappa_b} - (C^2 - V^2)C_be^{-i\kappa_b} + C(C^2+V^2)e^{-i\kappa}$. We see that the transmission vanishes at a certain nontrivial wave number value $\kappa_F = \cos^{-1}(-V^2C^{-2}/2)$, which corresponds to a Fano resonance [31,32]. At resonance, the reflection amplitude can be simply expressed as $R(\kappa_F) = -\exp(i\kappa_F)$. In order to use the Fano resonance to trap light in the resonator region, it is necessary to also satisfy the Fabry-Perot condition for one round-trip of the plane wave between the edge of the chain and the AW. This condition is obtained by enforcing the field relations at the right boundary ($n = 1$), leading to $\exp(-iN\kappa_F) + R\exp(iN\kappa_F) = 0$, and accordingly

$$(2N+1)\kappa_F = 2\pi m, \tag{3}$$

where m is an integer. We see that the Fano and Fabry-Perot resonance conditions are satisfied simultaneously when $V^2 = -2C^2\cos[2\pi m/(2N+1)]$. For the case of equal coupling $V = C$, we have $\kappa_F = 2\pi/3$, and the combined Fano and Fabry-Perot resonances occur for the number of waveguides in the resonator region $N = (3m-1)/2 = 1, 4, 7, \ldots$, corresponding to $m = 1, 3, 5, \ldots$.

In the following, the case $V = C$ and $N = 4$ is studied numerically and experimentally. For the experimental study, the waveguide array has to be finite, and we consider an array with total $J = 49$ waveguides (48 waveguides in the 1D chain plus the AW). We first consider the case of a homogeneous coupling in the waveguide array $C_b = C$ and numerically calculate the spectrum of eigenmodes from Eq. (1) by a stationary field approach. The allowed spectrum of propagation constants is presented in Fig. 2(a). We find extended eigenstates with eigenvalues $\beta \in [-2C, 2C]$ representing a quasicontinuum. Furthermore, as indicated by arrows in the figure we identify two localized states, which arise from the coupling of the AW with the 1D chain. The state indicated by a red arrow is a defect state residing inside the gap above the band of eigenvalues, and it is thus exponentially localized ($\beta = 2.38C$). The second state, indicated by the blue arrow, occurs at the eigenvalue corresponding to the Fano resonance, as it has a fundamentally different field structure with the zero amplitude in the background; i.e., this state strictly exists only between the edge and the AW. This property is referred to as "compactness." Furthermore, the propagation constant of this Fano-compact state (FCS) resides inside the allowed propagation band. The Fano resonance does not break up the band of eigenvalues of the unperturbed 1D chain, which makes the FCS a bound state in the quasicontinuum of the 1D chain. The vanishing of the electric field in waveguides $n = 5, 6, 7, \ldots$ does not allow any interaction of the FCS with the residual lattice. Therefore, the state is completely insensitive to the lattice structure in the background. Hence, the FCS does not change if C_b or the number of waveguides in the background is varied.

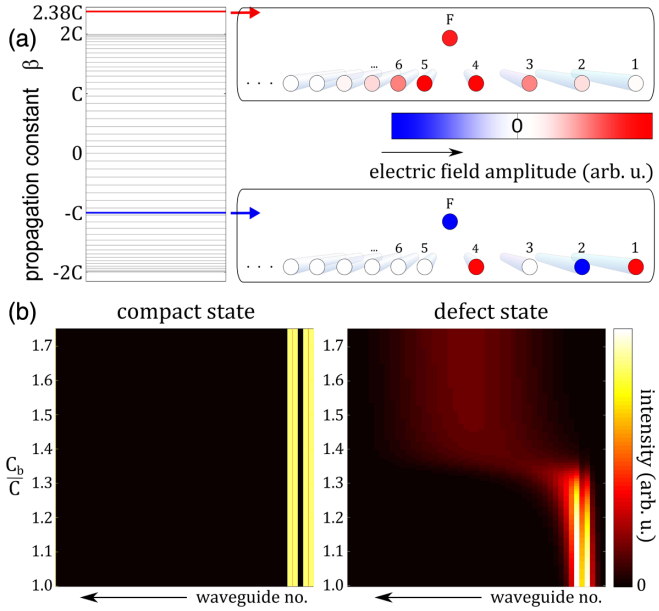

FIG. 2 (color online). (a) Eigenvalue spectrum of a structure with 49 homogeneously coupled waveguides ($C_b = V = C$). The amplitude profiles of the exponentially localized defect state (upper row) and the FCS (lower row) are shown on the right. (b) The profile of FCS (left) and defect state (right) as functions of C_b. The limit where the exponentially localized state ceases to exist is $C_b^{\mathrm{cr}} = 1.36C$. For $C_b \geq C_b^{\mathrm{cr}}$, the defect state is absorbed in the quasicontinuum and, hence, spreads over the entire array.

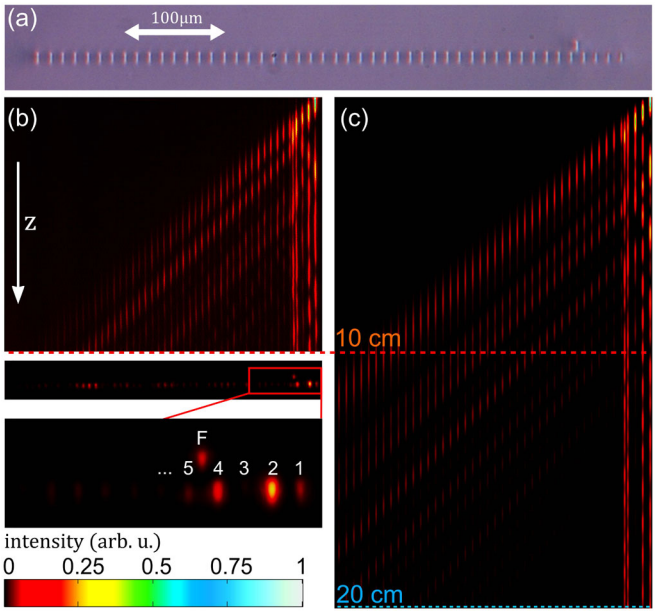

FIG. 3 (color online). (a) Microscope image of the front facet of the processed fused silica sample serving as the experimental realization of the structure. (b) Corresponding fluorescence microscopy measurement and the near-field image of the output facet. (c) Computed intensity evolution for 20 cm of propagation. The fluorescence images are normalized to their respective peak value.

Figure 2(b) demonstrates the change of the FCS (left) and the defect state (right) with increasing C_b. By an increase of $C_b \geq C$ the propagation band broadens until the exponentially localized state is absorbed into the band, whereas the FCS remains unchanged at $\beta = -C$. The critical ratio of the coupling constants for which the exponentially localized state ceases to exist is $C_b^{\mathrm{cr}}/C \simeq 1.36$.

A light beam coupled to the waveguide array will excite a superposition of different modes. The amplitudes of eigenstates will be proportional to the overlap of their spatial profiles with the input field distribution. For a single-waveguide excitation of the first site in the above structure, the amount of intensity dedicated to the FCS is 25%. The defect state is only excited with a fraction of 0.37% of the input intensity when $C_b = C$, and this decreases further when $C_b > C$.

For our experiments, we fabricated several waveguiding structures in fused silica using the femtosecond laser direct-writing approach [33]. The samples are 10 cm long, which is the maximum length feasible with our current fabrication technology. The experimental investigations now deal with two separate issues: first, observing the Fano resonance in an array with homogeneous coupling in the entire structure; second, proving the compactness of the FCS by varying the coupling constant C_b in the background. In order to directly observe the light evolution inside the structures we employ a fluorescence microscopy technique [34]. Among the possible single-waveguide excitations, the excitation of the first waveguide at the edge of the structure has the largest overlap with the FCS compared to the overlap with the defect state. In our experiments, linearly polarized light oriented along the x direction at $\lambda = 633$ nm is launched into this waveguide using a fiber butt coupling. In a first set of experiments, the spacing between neighboring waveguides of the chain is fixed to 13 μm, such that $C_b = C$. This results in a coupling of about $C = 0.2\ \mathrm{mm}^{-1}$. Figure 3(a) shows the microscope image of the front facet of the fabricated array. Because of the strongly elliptical shape of the waveguides, resulting from the fabrication process, the coupling strength depends not only on the separation of the waveguides but also on their orientation with respect to the coupling direction [35]. The vertical offset (h) of the AW with respect to the chain was carefully tuned in the experiment to match the condition $V = C$. For $\lambda = 633$ nm, equal coupling was achieved for $h = (\sqrt{3}d/2 + 2.6)$ μm. The experiments show that the resonance already disappears at $h \pm 0.5$ μm, indicating a high sensitivity to deviations from the resonance condition $C = V$. Changing the wavelength λ would also lead to $V \neq C$. The experimental data are shown in Fig. 3(b). When launching light into the edge waveguide of the structure, several eigenstates of the system are excited, including the FCS. Because of the reflection at the defect caused by the AW, the light carried by the extended eigenstates is transmitted gradually into

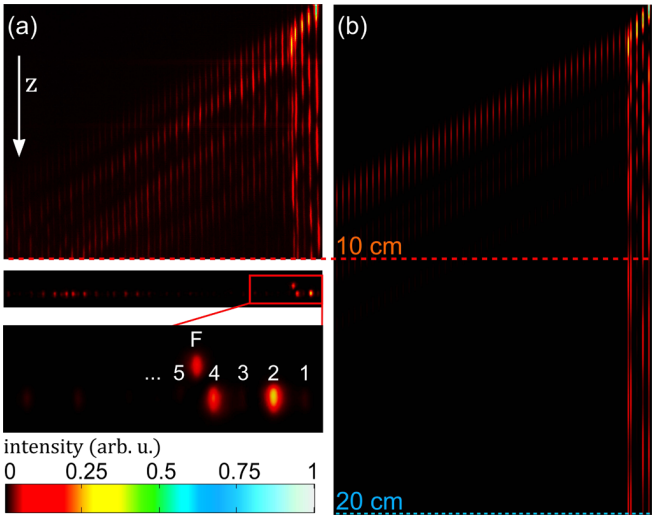

FIG. 4 (color online). Light evolution in a structure, where the coupling in the background region is increased to $C_b/C = 1.75$. (a) Fluorescence microscopy measurement and the near-field image of the output facet. (b) Computed intensity evolution for 20 cm of propagation. Only the fluorescence images are normalized to their respective peak value.

the background. After 10 cm of propagation, the intensity pattern in the resonator region is not perfectly reduced to the intensity pattern of the FCS. The transient behavior within the first five waveguides still includes intensity oscillations in each waveguide. However, the output pattern already exhibits the characteristic "dark" third waveguide [Fig. 3(b), lower part] identifying the FCS. The simulations, shown in Fig. 3(c), confirm the measured behavior. The simulations are obtained by solving the system of coupled differential equations Eq. (1) numerically. In the plot of Fig. 3(c), each of the discrete amplitudes $|\psi_i(z)|^2$ was dressed with a Gaussian function to facilitate the comparison with the fluorescence image. Even after 20 cm of propagation, the FCS is not established perfectly, but the data in Fig. 3 are sufficient to confirm the existence of the FCS. In the next experiment, we aim to demonstrate the compactness of the FCS. To this end, in a second sample we reduced the spacing in the background region to 11 μm, which corresponds to $C_b \approx 0.35$ mm^{-1}, whereas in the region close to the surface 13 μm spacing is reproduced. Therefore, the Fano resonance is expected at a similar height h of the AW, compared to the first structure. Indeed, $V = C$ was here achieved for $h = (\sqrt{3}d/2 + 2.2)$ μm. The experimental data in Fig. 4(a) show that an intensity distribution in the first five waveguides evolves to a final state that is very similar to that observed in the first experiment; cf. Fig. 3(a). Our simulations of the light evolution in this structure [Fig. 4(b)] confirm this trend. This is the experimental confirmation that the FCS is independent of the topology of the background region of the 1D waveguide chain and, thus, the FCS is compact. Nevertheless, the transient behavior changes slightly. This is reasonable since the occupation of the eigenmodes has changed and, except for the FCS, the profiles of eigenmodes are sensitive to the value of C_b.

In conclusion, we have theoretically predicted and experimentally demonstrated the existence of a compact bound state in the continuum of a one-dimensional waveguide array. This state is confined to a finite region of the array and exhibits no exponentially decaying tails. We found the condition when all localized states other than the compact state ceased to exist. Our results may pave the way for various applications for, e.g., telecommunication (where the resonance can be used to transmit information only at the surface of the optical communication channel), mode filtering (where the coupling between the AW and the lattice is changed in order to change the energy of the BIC), and surface sensing (where the BIC can be used to detect distortions at the edge of a system).

This work was support by the Australian Research Council through Future Fellowship program (including FT100100160 and FT110100037) and Discovery Project No. DP130100086, the German Ministry of Education and Research (Center for Innovation Competence programme, Grant No. 03Z1HN31), and the Thuringian Ministry for Education, Science and Culture (Research group Spacetime, Grant No. 11027-514). R. Keil was supported by the Abbe School of Photonics. Y. X. acknowledges the support from the NNSF of China (Grant No. 11304047) and the Nonlinear Physics Centre at ANU for their hospitality.

[1] *Electromagnetic Surface Modes*, edited by A. D. Boardman (Wiley, New York, 1982).
[2] S. A. Maier, *Plasmonics: Fundamentals and Applications* (Springer, New York, 2007).
[3] M. I. D'yakonov, Sov. Phys. JETP **67**, 714 (1988).
[4] I. E. Tamm, Phys. Z. Sowjetunion **1**, 733 (1932).
[5] J. von Neumann and E. Wigner, Z. Phys. Chem., Abt. A **30**, 465 (1929).
[6] F. H. Stillinger and D. R. Herrick, Phys. Rev. A **11**, 446 (1975).
[7] H. Friedrich and D. Wintgen, Phys. Rev. A **32**, 3231 (1985).
[8] F. Capasso, C. Sirtori, J. Faist, D. L. Sivco, S.-N. G. Chu, and A. Y. Cho, Nature (London) **358**, 565 (1992).
[9] G. Ordonez, K. Na, and S. Kim, Phys. Rev. A **73**, 022113 (2006).
[10] S. Longhi, Eur. Phys. J. B **57**, 45 (2007).
[11] Q. F. Xu, P. Dong, and M. Lipson, Nat. Phys. **3**, 406 (2007).
[12] D. C. Marinica, A. G. Borisov, and S. V. Shabanov, Phys. Rev. Lett. **100**, 183902 (2008).
[13] E. N. Bulgakov and A. F. Sadreev, Phys. Rev. B **78**, 075105 (2008).
[14] F. Dreisow, A. Szameit, M. Heinrich, T. Pertsch, S. Nolte, A. Tünnermann, and S. Longhi, Phys. Rev. Lett. **101**, 143602 (2008).
[15] S. Longhi, J. Mod. Opt. **56**, 729 (2009).

[16] E. N. Bulgakov and A. F. Sadreev, Phys. Rev. B **80**, 115308 (2009).
[17] C. R. Otey, M. L. Povinelli, and S. H. Fan, Appl. Phys. Lett. **94**, 231109 (2009).
[18] E. N. Bulgakov and A. F. Sadreev, Phys. Rev. B **81**, 115128 (2010).
[19] G. Rajput, P. K. Ahluwalia, and K. C. Sharma, Europhys. Lett. **94**, 17 003 (2011).
[20] A. Lovera, B. Gallinet, P. Nordlander, and O. J. F. Martin, ACS Nano. **7**, 4527 (2013).
[21] Q. F. Xu, B. Zhen, J. Lee, S. G. Johnson, J. D. Joannopoulos, and M. Soljacic, Nature (London) **499**, 188 (2013).
[22] Y. Plotnik, O. Peleg, F. Dreisow, M. Heinrich, S. Nolte, A. Szameit, and M. Segev, Phys. Rev. Lett. **107**, 183901 (2011).
[23] M. I. Molina, A. E. Miroshnichenko, and Y. S. Kivshar, Phys. Rev. Lett. **108**, 070401 (2012).
[24] U. Fano, Phys. Rev. **124**, 1866 (1961).
[25] B. Luk'yanchuk, N. I. Zheludev, S. A. Maier, N. J. Halas, P. Nordlander, H. Giessen, and C. T. Chong, Nat. Mater. **9**, 707 (2010).
[26] A. E. Miroshnichenko, S. Flach, and Y. S. Kivshar, Rev. Mod. Phys. **82**, 2257 (2010).
[27] J. Pan, Y. Huo, K. Yamanaka, S. Sandhu, L. Scaccabarozzi, R. Timp, M. L. Povinelli, S. Fan, M. M. Fejer, and J. S. Harris, Appl. Phys. Lett. **92**, 103114 (2008).
[28] J. Pan, S. Sandhu, Y. Huo, N. Stuhrmann, M. L. Povinelli, J. S. Harris, M. M. Fejer, and S. Fan, Phys. Rev. B **81**, 041101 (2010).
[29] J. Pan, Y. Huo, S. Sandhu, N. Stuhrmann, M. L. Povinelli, J. S. Harris, M. M. Fejer, and S. Fan, Appl. Phys. Lett. **97**, 101102 (2010).
[30] Y. Tanaka, J. Upham, T. Nagashima, T. Sugiya, T. Asano, and S. Noda, Nat. Mater. **6**, 862 (2007).
[31] A. E. Miroshnichenko, S. F. Mingaleev, S. Flach, and Y. S. Kivshar, Phys. Rev. E **71**, 036626 (2005).
[32] Y. Xu, A. E. Miroshnichenko, and A. S. Desyatnikov, Opt. Lett. **37**, 4985 (2012).
[33] A. Szameit and S. Nolte, J. Phys. B **43**, 163001 (2010).
[34] A. Szameit, F. Dreisow, H. Hartung, S. Nolte, A. Tuennermann, and F. Lederer, Appl. Phys. Lett. **90**, 241113 (2007).
[35] A. Szameit, F. Dreisow, T. Pertsch, S. Nolte, and A. Tuennermann, Opt. Express **15**, 1579 (2007).